# Downregulation of Glt25d1 aggravates carbon tetrachloride-induced acute hepatic injury through activation of the TGF-β1/Smad2 signaling pathway

XIAOHUI YE[1*], LINGLING HE[2*], JIALI MA[2], YUFENG LI[3], MANKA ZHANG[4], JUNRU YANG[2], JIAN ZHANG[4], FAN XIAO[5] and HONGSHAN WEI[1,2]

[1]Department of Gastroenterology, Peking University Ditan Teaching Hospital; [2]Department of Gastroenterology, Beijing Ditan Hospital, Capital Medical University, Beijing 100015; [3]Department of Gastroenterology, Beijing Changping Hospital, Beijing 100085; [4]Department of Center of Integrated Traditional Chinese and Western Medicine, Peking University Ditan Teaching Hospital; [5]Department of Institute of Infectious Disease, Beijing Ditan Hospital, Capital Medical University, Beijing 100015, P.R. China

Received December 24, 2017; Accepted May 16, 2018

DOI: 10.3892/mmr.2018.9392

**Abstract.** Collagen β (1-O) galactosyltransferase 1 (GLT25D1) has been reported to transfer galactose to hydroxylysine residues via β (1-O) linkages in collagen. The present study investigated the function of the collagen galactosyltransferase activity of GLT25D1 against carbon tetrachloride ($CCl_4$)-induced acute liver injury *in vitro*. Glt25d1$^{+/-}$ mice and wild-type (WT) mice were injected intraperitoneally with the same dose of $CCl_4$. The grade of hepatic injury and the extent of hepatocyte necrosis in the acute phase were assessed 48 h following $CCl_4$ injection. Hepatocyte necrosis was evaluated by histological examination and by serum alanine aminotransferase and aspartate aminotransferase levels, which were higher in the Glt25d1$^{+/-}$ mice compared with those in the WT mice. Reverse transcription-quantitative polymerase chain reaction was performed, and the results demonstrated that the mRNA expression levels of inflammatory cytokines, including tumor necrosis factor-α and interleukin-6 were significantly increased in the Glt25d1$^{+/-}$ mice. Furthermore, western blot analyses were performed, and the results demonstrated that the protein levels of cleaved caspase-3 and -9 were also markedly increased in the Glt25d1$^{+/-}$ liver, indicating that hepatocyte apoptosis was induced. Additionally, the expression levels of transforming growth factor (TGF)-β1 and phosphorylated small mothers against decapentaplegic (Smad)2 were markedly upregulated, indicating activation of the TGF-β1/Smad2 signaling pathway during $CCl_4$-induced acute liver injury in Glt25d1$^{+/-}$ mice. $CCl_4$ administration also resulted in severe damage to Glt25d1$^{+/-}$ primary hepatocytes *in vitro*. Taken together, the downregulation of Glt25d1 deteriorated $CCl_4$-induced liver injury in mice, which may involve triggering inflammatory responses, apoptosis and TGF-β1/Smad2 signaling pathway activation.

*Correspondence to:* Professor Hongshan Wei, Department of Gastroenterology, Beijing Ditan Hospital, Capital Medical University, 8 East Jingshun Street, Chaoyang, Beijing 100015, P.R. China
E-mail: drwei@ccmu.edu.cn

*Contributed equally

*Key words:* acute hepatic injury, inflammation, apoptosis, collagen β (1-O) galactosyltransferase 1, transforming growth factor-β1/small mothers against decapentaplegic 2

## Introduction

Liver injury has been recognized as a serious health problem worldwide (1) and can be caused by toxic chemicals, drugs or alcohol abuse, viral infection and other factors (2,3). However, the mechanisms underlying liver injury remain to be fully elucidated (4) and few effective therapies are available for acute liver injury at present. Therefore, it is necessary to elucidate the possible molecular mechanism underlying liver injury for developing effective drugs. The collagen β (1-O) galactosyltransferase 1 (*Glt25d1*) gene encodes Hyl-specific galactosyltransferase enzymes, which catalyze the transfer of β-linked Gal to Hyl residues on collagen (5,6), which initiates collagen glycosylation during its post-translational modification. Despite the identification of Glt25d1, its functional role in collagen glycosylation remains to be fully elucidated. The biological significance of collagen glycosylation also remains to be elucidated as it has neither been associated with a disease nor has a model organism harboring defective collagen glycosylation been described to date (7,8).

Previous studies have indicated that transgenic mice with mutations that caused cytoskeletal keratin lacking of glycosylation modifications in the extracellular matrix (ECM) are susceptible to liver injury (8,9) and that glycosyltransferase activities in the extracellular space are important for cell growth and viability (10). Accordingly, in the present study, Glt25d1$^{+/-}$ mice, lacking one allele of *Glt25d1*, were

established, and their susceptibility to liver injury induced by carbon tetrachloride ($CCl_4$) was compared with that of wild-type (WT) mice.

## Materials and methods

*Animals and treatments*. To examine the functional roles of Glt25d1 *in vivo*, a Glt25d1 conventional knockout mouse model was established ($Glt25d1^{flox/flox}$) with loxP sites flanking exons 2 and 3 of the Glt25d1 gene. The $Glt25d1^{flox/flox}$ mice were crossed with CMV-Cre transgenic mice, both of which were purchased from the Model Animal Research Center Of Nanjing University (Nanjing, China), to facilitate the deletion of exons 2 and 3 of Glt25d1 and generate heterozygous Glt25d1 mice ($Glt25d1^{+/-}$). This targeted disruption results in a frame shift mutation, which leads to the early termination of GLT25D1 protein translation. However, no homozygous $Glt25d1^{-/-}$ mice were recovered from the intercrossed $Glt25d1^{+/-}$ mice, which suggested that a lack of functional Glt25d1 alleles resulted in embryonic lethality.

A total of 14 female $Glt25d1^{+/-}$ mice, 7-8 weeks of age and 18-20 g in weight, were fed in a specific pathogen-free laboratory environment, with free access to standard pellet chow and sterile water. Mice were housed at the Department of Laboratory Animal Science, Peking University Health Science Center (Beijing, China), and maintained under a 12/12 h light/dark cycle, an ambient temperature of 21±2˚C and a constant humility of 50±10%. C57BL/6J WT mice of the same age, gender and weight served as controls. The mice were divided into four groups (n=6-8/group). Acute liver injury model groups ($Glt25d1^{+/-}$ and WT) were injected intraperitoneally with a single dose of $CCl_4$ [10 ml/kg body weight dissolved in corn oil (1:6)] as reported previously (11). The WT control and $Glt25d1^{+/-}$ control mice were administered the same dose of corn oil without $CCl_4$. Subsequently, all mice were sacrificed 48 h following $CCl_4$ injection. Blood and liver samples were collected for further analyses. All experimental procedures were performed according to the Animal Care Committee guidelines and the experimental protocol was approved by the Ethics Committee of Peking University Health Science Center.

*Alanine aminotransferase (ALT) and aspartate aminotransferase (AST) assessment*. Serum samples were separated from the blood by centrifugation at 3,000 x g for 10 min at 4˚C. Serum AST and ALT levels were determined using a biochemical kit (Sichuan Maccura Biotechnology, Sichuan, China).

*Hematoxylin/eosin (HE) staining*. The liver tissues were excised, fixed in 10% formalin, paraffin-embedded, cut into 4-$\mu$m sections, and stained with HE according to a standard protocol. All the images were acquired and analyzed using an Axio Observer A1 Fluorescence Microscope (ZeissAG, Oberkochen, Germany). Six randomly selected fields (magnification, x100) were assessed for necrosis according to standard morphological criteria, including loss of architecture and morphological changes in the cells, and the necrotic area percentage was determined as reported previously (12).

*Reverse transcription-quantitative polymerase chain reaction (RT-qPCR) analysis*. Total RNA was extracted from the liver tissue using the TRIzol reagent protocol (Takara Biotechnology Co., Ltd., Dalian, China). The concentration and quantity of isolated total RNA was determined using NanoDrop One Microvolume UV-Vis Spectrophotometer (Thermo Fisher Scientific, Inc., Waltham, MA, USA). Reverse transcription was performed using a PrimeScript RT Reagent kit (Takara Biotechnology Co., Ltd.) under the following conditions: 37˚C for 15 min, 85˚C for 5 sec and then maintained at 4˚C. RT-qPCR was performed in a 20 $\mu$l reaction volume [diluted cDNA (2 $\mu$l), primers (0.4 $\mu$l per primer), SYBR Premix EX Taq (10 $\mu$l; Promega Corporation, Madison, WI, USA) and nuclease-free water (7.2 $\mu$l)]. qPCR was performed using a Tetrad2 Peltier Thermal Cycler (Bio-Rad Laboratories, Inc., Hercules, CA, USA) and the reaction was run on an Applied Biosystems 7500 Real-Time PCR system under the following conditions: i) holding stage: 95˚C for 2 min; ii) cycling stage: 95˚C for 15 sec, 60˚C for 1 min, (40 cycles); iii) melt curve stage: 95˚C for 15 sec, 60˚C for 1 min, 95˚C for 30 sec, 60˚C for 15 sec. *Gapdh* was amplified as a reference gene and differences between the relative expression of the target genes were calculated using the $2^{-\Delta\Delta Cq}$ method (13). The sequences of the primers used for PCR are shown in Table I.

*Western blot analysis*. Total proteins were extracted from the liver using T-PER™ Tissue Protein Extraction reagent (Thermo Fisher Scientific, Inc., Waltham, MA, USA; cat. no. 78510) and the protein concentration in samples was measured using the Pierce™ BCA Protein Assay kit (Thermo Fisher Scientific, Inc.; cat. no. 23227). An equivalent quantity of protein (80 $\mu$g) was loaded onto SDS-polyacrylamide gels (10%), electrophoresed and then transferred onto Immobilon® PVDF membranes (Sigma; EMD Millipore, Billerica, MA, USA; cat. no. P3313). Following this, the membranes were blocked for 2 h at room temperature using Tris-buffered saline containing 0.1% Tween 20 and 5% skimmed milk at room temperature. The following primary antibodies were used: Monoclonal rabbit anti-mouse GAPDH (Cell Signaling Technology, Inc., Danvers, MA, USA; cat. no. 5174, 1:1,000), polyclonal rabbit anti-mouse caspase-3 (Cell Signaling Technology, Inc.; cat. no. 9662, 1:1,000), polyclonal rabbit anti-mouse Glt25d1 (ProteinTech Group, Inc., Chicago, IL, USA; cat. no. 16768-1-AP, 1:1,000), monoclonal rabbit anti-mouse caspase9 (Abcam, Cambridge, UK; cat. no. ab202068, 1:500), polyclonal rabbit anti-mouse TGF-β1 (ProteinTech Group, Inc.; cat. no. 21898-1-AP, 1:1,000), monoclonal rabbit anti-mouse phosphorylated (p)-Smad2/3 (Cell Signaling Technology, Inc.; cat. no. 8828, 1:1,000) and polyclonal rabbit anti-mouse Smad2 (ProteinTech Group, Inc.; cat. no. 12570-1-AP, 1:1,000) at 4˚C overnight. This was followed by incubation with the goat anti-mouse (Abcam; cat. no. ab6789, 1:5,000) and anti-rabbit secondary antibodies (Abcam; cat. no. ab191866, 1:5,000) for 2 h at room temperature. The sample bands were revealed using the Tanon Imaging system (Tanon Science and Technology Co., Ltd., Shanghai, China).

*Isolation and culture of mouse primary hepatocytes*. Mouse primary hepatocytes were isolated from the female WT

Table I. Primer sequences for reverse transcription-quantitative polymerase chain reaction analysis.

| Gene (ID) | Primer sequence (5'-3') |
|---|---|
| *Tnf-α* | Forward: TGGGCCTCTCATGCACCACC |
| | Reverse: GAGGCAACCTGACCACTCTCCCT |
| *Il-6* | Forward: AGACAAAGCCAGAGTCCTTCAG |
| | Forward: GCCACCTTTTGACAGTGATGAG |
| *Il-1β* | Forward: GCCACCTTTTGACAGTGATGAG |
| | Reverse: GACAGCCCAGGTCAAAGGT |
| *Gapdh* | Forward: CAATGACCCCTTCATTGAC |
| | Reverse: GATCTCGCTCCTGGAAGATG |

*Tnf-α*, tumor necrosis factor-α; *Il-6*, interleukin-6; *Il-1β*, interleukin-1β.

or Glt25d1$^{+/-}$ mice using a two-step collagenase perfusion procedure as described previously (14). The hepatocytes were purified further using 60% percoll (1.076 g/ml) (15,16). The mean viability and purity of mouse primary hepatocytes following isolation were identified by trypan blue exclusion and periodic acid Schiff (PAS) staining, respectively. All the images were acquired and analyzed using an Axio Observer A1 Fluorescence Microscope (Zeiss AG). Low activity or dead hepatocytes were stained blue by trypan blue staining. Six fields (original magnification, x100) were selected randomly and the ratio of hepatocellular viability was calculated according to the following formula: Cell viability=1-(number of blue cells/total number of cells) x100%. The hepatocytes were subjected to PAS staining, which specifically stains the hepatocyte cytoplasm red, in order to assess their purity. Six fields (original magnification, x100) were selected randomly and the ratio of hepatocellular purity was calculated according to the following formula: Hepatocellular purity=(number of red cells/total number of cells) x100%.

*Induction of hepatocyte death/apoptosis*. The cells were plated in 96-well plates at a density of 30,000 cells/well and cultured in high-glucose Dulbecco's Modified Eagle Medium (cat. no. 10569010; Gibco; Thermo Fisher Scientific, Inc.) supplemented with 10% fetal bovine serum (cat. no. 10100l47; Gibco; Thermo Fisher Scientific, Inc.) and 1% penicillin-streptomycin (cat. no. 1037806; Gibco; Thermo Fisher Scientific, Inc.) under a humidified atmosphere of 5% $CO_2$ at 37˚C for 24 h. Following this, the cells were used for the experiments and divided into the following groups: Groups 1 and 2 (normal control): Culture media were removed and cells were treated with 100 $\mu$l of serum-free medium for 2 h. A further 100 $\mu$l of serum-free medium was then added for the following 24 h; groups 3 and 4 ($CCl_4$ treatment): Culture media were removed, and the cells were treated with 100 $\mu$l of serum-free medium for 2 h. A further 100 $\mu$l of serum-free medium containing $CCl_4$ at the selected concentration (1% v/v) (17) was added for the following 24 h. $CCl_4$ cytotoxicity was determined using a CCK-8 assay kit. The cells were treated with CCK-8 reagent (10 $\mu$l/well) and incubated for a further 3-4 h. The optical density (OD) was recorded at 450 nm in a microplate reader (Thermo Fisher Scientific, Inc.). The ratio of cell survival (%) was determined using the following equation: Cell survival (%)=[OD(s)-OD(b)/OD(c)-OD(b)] x100%. OD(s), OD(b) and OD(c) represent the absorbance values of the sample, blank and negative control, respectively.

*Statistical analysis*. Quantitative data are expressed as the mean ± standard deviation, and statistical evaluation was performed using SPSS 18.0 statistical software (SPSS, Inc., Chicago, IL, USA). Significance was determined by Student's t-test or two-way analysis of variance followed by Tukey's test. P<0.05 was considered to indicate a statistically significant difference.

## Results

*Downregulation of Glt25d1 aggravates $CCl_4$-induced hepatic injury*. As shown in Fig. 1A-D, the HE staining showed severe hepatocyte degeneration and necrosis at the centrilobular zones at 48 h post-$CCl_4$ administration. The Glt25d1$^{+/-}$ mice exhibited larger annular necrotic lesion areas around the hepatic lobule portal area compared with the WT mice (0.48±0.10, vs. 0.22±0.06, P<0.01) as shown in Fig. 1E (arrows indicate lesions) and exhibited bridging necrosis. The above results were supported by a higher increase of serum ALT and AST levels in the Glt25d1$^{+/-}$ mice compared with the WT mice (P<0.001; Fig. 1F and G). For further confirmation of these results, the mRNA expression of inflammatory cytokines was examined. $CCl_4$ treatment caused elevated expression of *Tnf-α*, *Il-6* and *Il-1β* in the livers of the WT mice, and the expression levels of *Tnf-α* and *Il-6* were increased further in the Glt25d1$^{+/-}$ mice (all P<0.05; Fig. 2A-C).

*Glt25d1 deficiency increases $CCl_4$-induced hepatocellular apoptosis*. The levels of the cleaved forms of caspase-3 and -9 in the Glt25d1$^{+/-}$ liver were significantly higher compared with those in the WT liver (P<0.001 and P<0.01, respectively; Fig. 3A-C).

*Activation of the TGF-β1/Smad2 signaling pathway in Glt25d1$^{+/-}$ mice*. Compared with the control mice, the model mice exhibited elevated levels of TGF-β1 and p-Smad2/Smad2. The upregulation of the TGF-β1/Smad2 signaling pathway in the Glt25d1$^{+/-}$ liver was more marked compared with that in the WT liver (P<0.001, Fig. 3A, D and E). $CCl_4$ treatment increased the protein level of Glt25d1 in the WT and Glt25d1$^{+/-}$ mice (P<0.05; Fig. 3A and F).

*Downregulation of Glt25d1 enhances $CCl_4$-induced cytotoxicity in mouse primary hepatocytes in vitro*. The morphology of mouse primary hepatocytes following initial plating and incubation for 4 h is shown respectively in Fig. 4A and B. Low activity or dead hepatocytes were positively stained by trypan blue (Fig. 4C). Six randomly selected fields (magnification, x100) were subsequently investigated, and the mean viability of primary hepatocytes was revealed to be >94.0% (data not shown). As presented in Fig. 4D, the purity of cultured hepatocytes was investigated

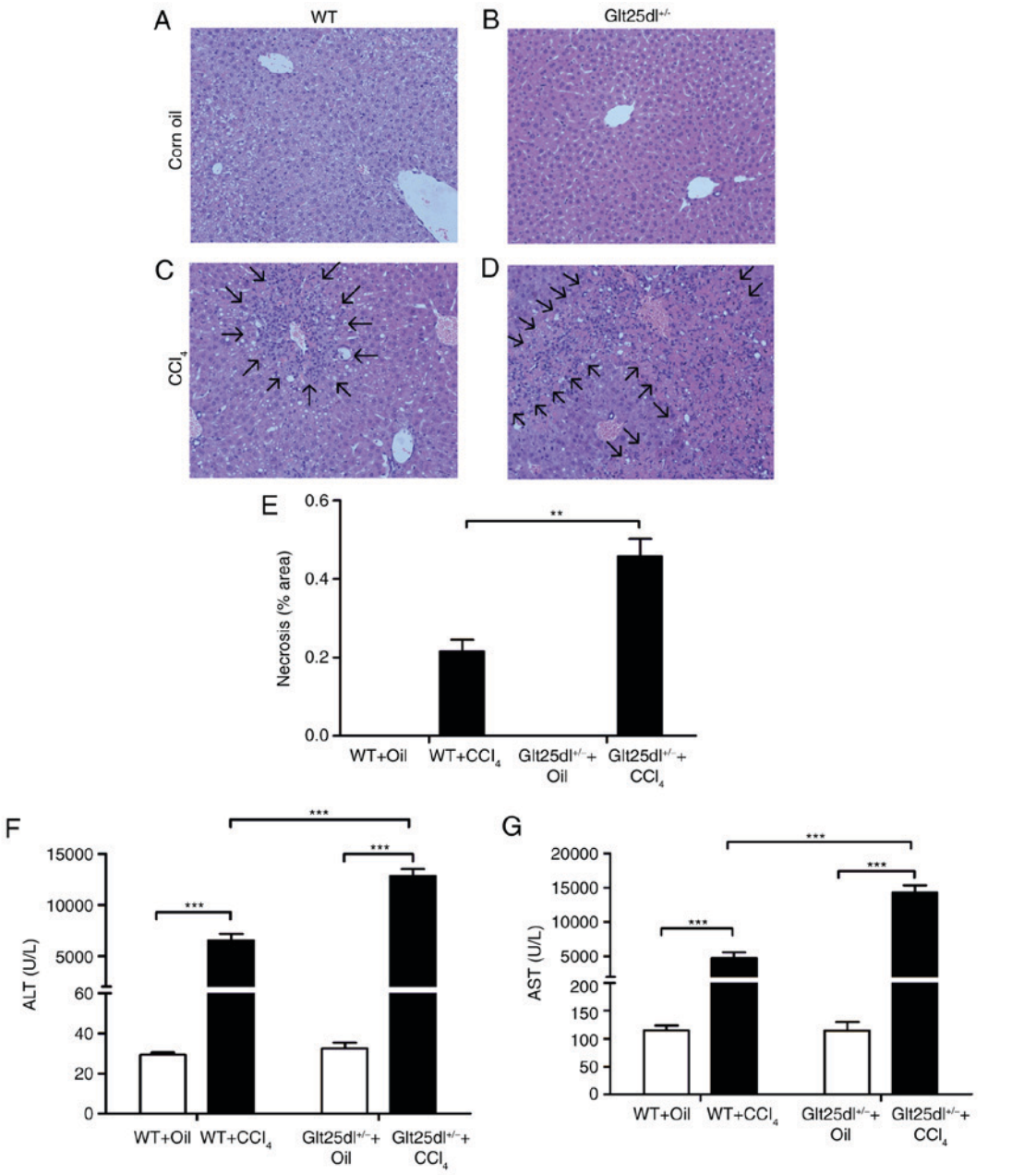


Figure 1. $CCl_4$ treatment aggravates hepatic necrosis in Glt25d1$^{+/-}$ mice. Representative micrographs of HE-stained liver sections from (A) WT and (B) Glt25d1$^{+/-}$ groups treated with corn oil and (C) WT and (D) Glt25d1$^{+/-}$ groups treated with $CCl_4$. Arrows indicate necrotic areas (magnification, x100). (E) Necrotic area percentages. Changes in serum (F) ALT and (G) AST levels in $CCl_4$- and corn oil-treated mice. Data are expressed as the mean ± standard deviation (n=6-8). $^{**}$P<0.01, $^{***}$P<0.001; significance determined by Student's t-test or two-way analysis of variance followed by Tukey's test. Glt25d1, collagen β (1-O) galactosyltransferase 1; $CCl_4$, carbon tetrachloride; ALT, alanine aminotransferase; AST, aspartate aminotransferase; WT, wild-type.

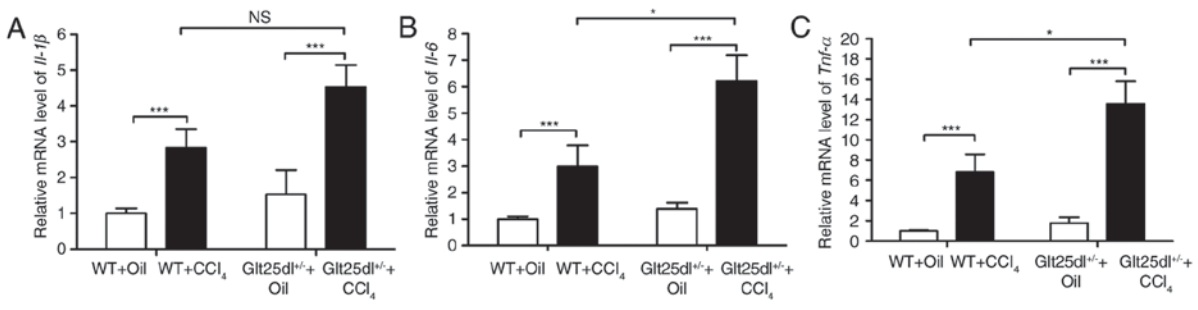


Figure 2. Glt25d1 deficiency upregulates the mRNA expression of inflammatory cytokines. Reverse transcription-quantitative polymerase chain reaction analysis evaluation of (A) *Il-1β*, (B) *Il-6* and (C) *Tnf-α* genes. Data are expressed as the mean ± standard deviation (n=4-6); $^{*}$P<0.05, $^{**}$P<0.01; significance determined by two-way analysis of variance followed by Tukey's test. Glt25d1, collagen β (1-O) galactosyltransferase 1; WT, wild-type; $CCl_4$, carbon tetrachloride; *Il-1β*, interleukin-1β; *Il-6*, interleukin-6; *Tnf-α*, tumor necrosis factor-α; NS, no significant difference.

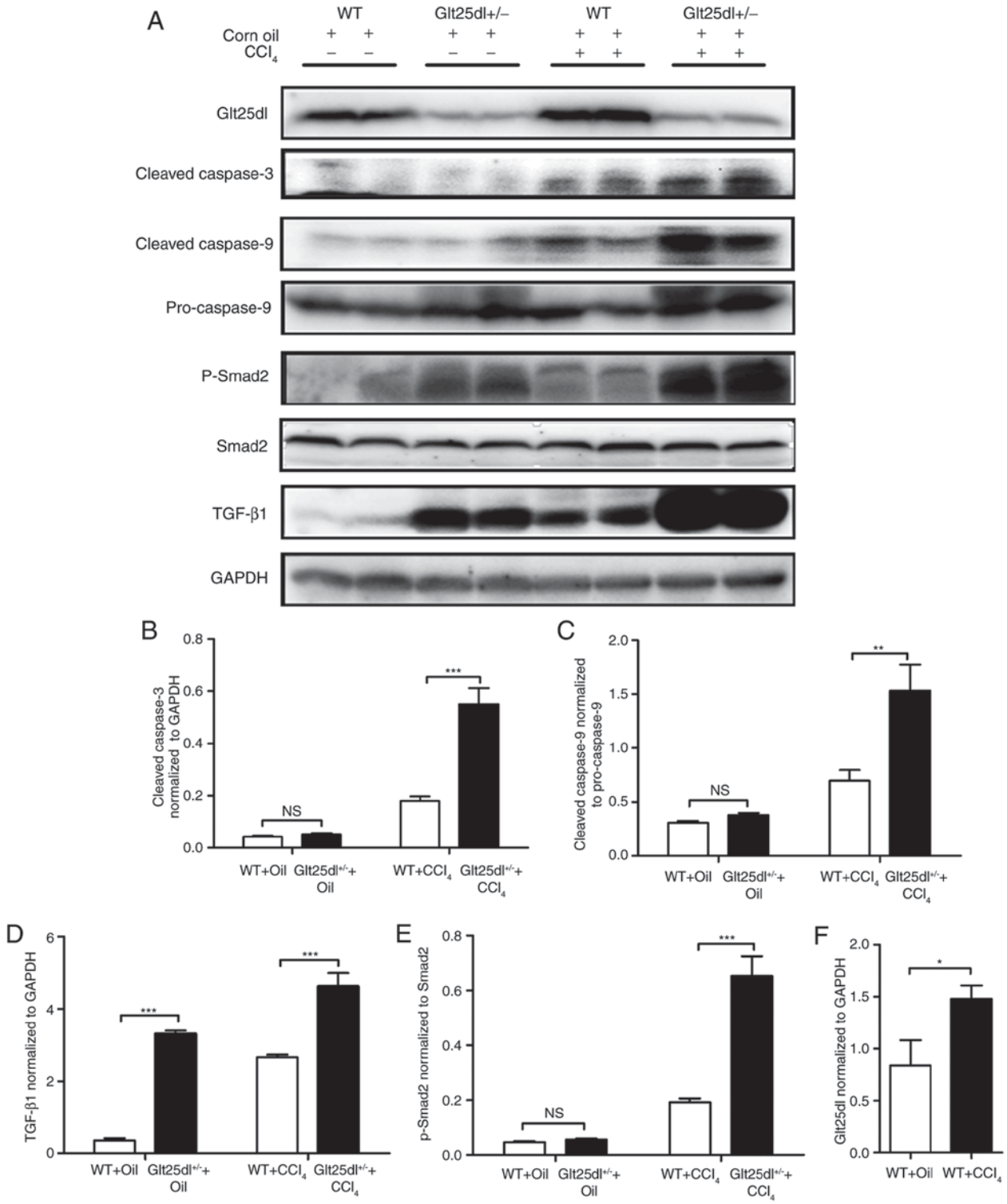


Figure 3. Apoptosis is severe and the TGF-β1/Smad2 signaling pathway is significantly activated in Glt25d1$^{+/-}$ mice. (A) Representative western blots of TGF-β, Glt25d1, cleaved caspase-3, cleaved caspase-9, caspase-9, p-Smad2/3 and Smad2 in the liver. Quantification of individual protein bands of (B) cleaved caspase-3, (C) cleaved caspase-9, (D) TGF-β, (E) p-Smad2 and (F) Glt25d1 were normalized to the corresponding GAPDH levels (n=6-8). $^{*}$P<0.05, $^{**}$P<0.01, $^{***}$P<0.001; significance determined by Student's t-test or two-way analysis of variance followed by Tukey's test. Glt25d1, collagen β (1-O) galactosyltransferase 1; $CCl_4$, carbon tetrachloride; WT, wild-type; TGF-β, transforming growth factor-β; Smad, small mothers against decapentaplegic; p-, phosphorylated; NS, not significant.

by PAS staining, which specifically stains the hepatocyte cytoplasm red. Following this, six randomly selected fields (magnification, x100) were investigated, and the mean purity of primary hepatocytes was revealed to be 96.25±1.20% (data not shown).

The Glt25d1$^{+/-}$ primary hepatocytes exhibited decreased viability upon treatment with 1% $CCl_4$. Compared with the WT cells, the Glt25d1$^{+/-}$ primary hepatocytes were more sensitive to $CCl_4$-induced toxicity and showed greater loss of viability (P<0.05; Fig. 4E).

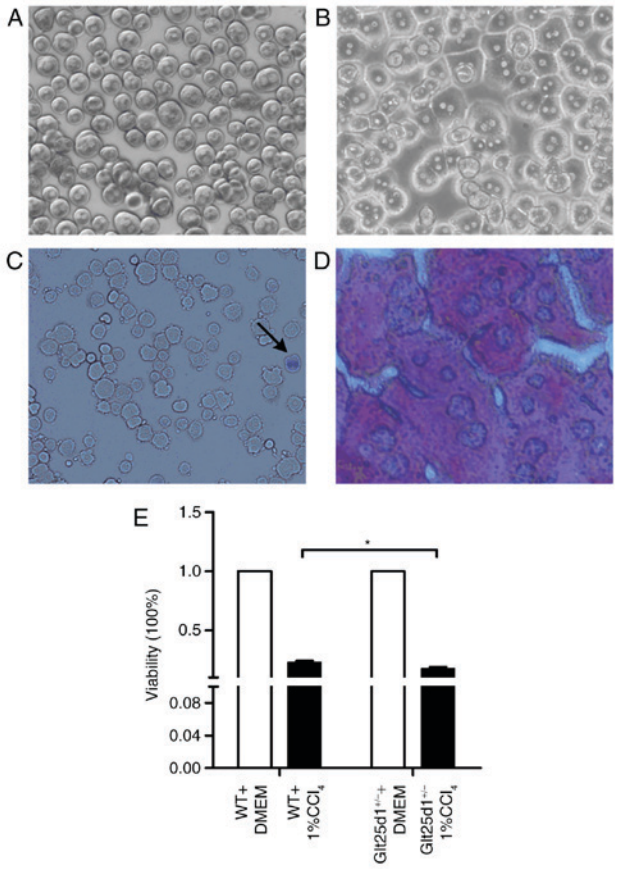


Figure 4. Glt25d1$^{+/-}$ primary hepatocytes show increased viability loss upon treatment with 1% $CCl_4$. (A) Morphology of mouse primary hepatocytes following initial plating (magnification, x100). (B) Morphology of mouse primary hepatocytes following incubation for 4 h (magnification, x100). (C) Viability of primary hepatocytes evaluated by trypan blue exclusion. The arrow indicates a dead cell (magnification, x100). (D) Purity of primary hepatocytes identified by PAS staining (magnification, x400). (E) Effects of 1% $CCl_4$ treatment for 24 h in primary hepatocytes. $^*P<0.05$; significance determined by Student's t-test. Glt25d1, collagen β (1-O) galactosyltransferase 1; $CCl_4$, carbon tetrachloride; WT, wild-type.

## Discussion

The present study demonstrated that Glt25d1$^{+/-}$ mice, which exhibited downregulated Glt25d1 synthesis, developed aggravated $CCl_4$-induced liver injury compared with WT mice *in vivo*. It also provided evidence suggesting that Glt25d1 deficiency may aggravate $CCl_4$-induced liver injury via TGF-β1/Smad2 signal pathway activation.

The ECM is known to have multiple biological functions, including cell self-renewal, adhesion, differentiation, proliferation and survival (18,19). Despite the well-regulated homeostasis of ECM components, particularly the level of collagen, which is important in tissue repair and remodeling (20,21), few studies have investigated the role of collagen glycosylation in the pathogenesis or resolution of acute liver injury. In 2009, Schegg *et al* (5) confirmed that collagen glycosylation during post-translational modification was catalyzed by Glt25d1 and Glt25d2 *in vitro*. Subsequent investigations have demonstrated that Glt25d1 is required for the secretion of high molecular weight adiponectin (6) and that Glt25d1 deletion induces collagen accumulation in osteosarcoma cells *in vitro* (7). The present study is the first, to the best of our knowledge, to examine the effect of Glt25d1 on acute liver injury *in vivo*.

The present study utilized $CCl_4$, a chemical hepatotoxin, to generate a classical animal model of acute hepatic injury (22,23) in Glt25d1$^{+/-}$ and WT mice. The results demonstrated that the Glt25d1$^{+/-}$ mice developed aggravated $CCl_4$-induced liver injury compared with the WT mice. HE staining of the Glt25d1$^{+/-}$ liver tissues showed severe hepatocyte degeneration and necrosis (Fig. 1D), which was supported by a higher increase in the levels of serum ALT and AST (Fig. 1E and G). These data also provided evidence that Glt25d1 had beneficial effects in reducing hepatic necrosis. Apoptosis or programmed cell death, particularly hepatocyte apoptosis, is a common feature of various liver diseases (24). Previous studies have reported severe hepatocyte apoptosis in $CCl_4$-induced acute liver injury (25,26). In order to evaluate the extent of liver tissue apoptosis in the present study, western blot analysis for cleaved caspase-3, cleaved caspase-9, and pro-caspase-9 was performed, which revealed that the apoptosis was more severe in the livers of the Glt25d1$^{+/-}$ than in the livers of the WT mice (Fig. 3A). It is well known that hepatocyte necrosis can recruit numerous inflammatory cells, which secrete cytokines, including TNF-α, IL-6 and IL-1β, and trigger an inflammatory response (27,28). In addition, evidence suggests that apoptosis is a pro-inflammatory and fibrogenic stimulus (29). Consistent with the above results, the mRNA levels of *Tnf-α* and *Il-6* were markedly increased in the livers of Glt25d1$^{+/-}$ mice in the present study (Fig. 2B and C), which indicated that normal collagen glycosylation may alleviate $CCl_4$-induced liver dysfunction. Hyaluronan (HA), a ubiquitous glycosaminoglycan, is another common component of the ECM (30). Consistent with the results of the present study, HA-knockout mice exhibited increased hepatic injury in $CCl_4$-induced acute liver injury (31). These results demonstrated that integrity and repair of the ECM is important in ameliorating liver injury.

Under the same $CCl_4$ treatment, Glt25d1$^{+/-}$ primary hepatocytes showed increased loss of viability *in vitro* (Fig. 4D), which was consistent with the results of Baumann and Hennet, who suggested that the complete loss of collagen glycosylation catalyzed by GLT25D1 and GLT25D2 impairs osteosarcoma cell proliferation and viability (7). This suggests that GLT25D1 deficiency may directly influence $CCl_4$-induced cytotoxicity in primary hepatocytes.

A number of studies have shown that the TGF-β1 signaling pathway is involved in the development of various diseases (32-34) and that activation of the TGF-β1/Smad signaling pathway may aggravate the severity of $CCl_4$-induced liver injury (35). To determine whether the glycosylation effect of GLT25D1 alleviates acute liver injury through TGF-β1 signaling pathways, the present study evaluated the protein levels of p-Smad2, Smad2 and GLT25D1 in the liver tissues. The results indicated that, upon $CCl_4$ administration, the protein expression levels of GLT25D1 and p-Smad2, and the ratio of p-Smad2/Smad2 were upregulated, compared with the control mice. In addition, activation of the TGF-β1/Smad2 signaling pathway was more marked in the Glt25d1$^{+/-}$mice. These data demonstrated that GLT25D1 deficiency may

aggravate $CCl_4$-induced liver injury through TGF-β1/Smad2 signaling pathway activation.

There were several limitations of the present study. Firstly, due to the embryonic lethality induced by conventional knockout, it was not possible to obtain Glt25d1$^{-/-}$ homozygous mice. In follow-up investigations on embryonic lethality, the Glt25d1$^{-/-}$ mouse embryos exhibited severe developmental arrest and usually died prior to embryonic day 13.5. To better understand the function of Glt25d1, the generation of liver-specific Glt25d1 mutant mice is underway.

Secondly, in order to evaluate $CCl_4$-induced hepatotoxicity in the WT and Glt25d1$^{+/-}$ primary hepatocytes *in vitro*, ALT, AST and lactate dehydrogenase require identification in the culture supernatants. These associated experiments are also underway.

In conclusion, using Glt25d1$^{+/-}$ mice, the present study demonstrated that Glt25d1 deficiency aggravated $CCl_4$-induced acute liver injury through activation of the TGF-β1/Smad2 signaling pathway. Although further investigation is required to elucidate the detailed mechanisms responsible for these observations, the role of Glt25d1 requires consideration for examining novel therapeutic strategies against acute liver injury.

**Acknowledgements**

The authors would like to thank Spandidos Publications for their English language editing.

**Funding**

This study was supported by grants from the National Natural Science Foundation of China (grant nos. 81271901 and 30671875), the Beijing Natural Science Foundation (grant no. 7152073) and the Science Foundation of Capital Medicine Development (grant no. 2014-2-2171) to Professor Hongshan Wei.

**Availability of data and materials**

Not applicable.

**Authors' contribution**

XY and LH performed the experiments and wrote the manuscript. JM, YL and MZ performed the experiments. JY and JZ helped to raise animals and established the animal model of acute liver injury. FX analyzed the data. HW designed the study and critically revised the manuscript for important intellectual content.

**Ethics approval and consent to participate**

All experimental procedures were performed according to the Animal Care Committee guidelines and the experimental protocol was approved by the Ethics Committee of Peking University Health Science Center.

**Patient consent for publication**

Not applicable.

**Competing interests**

The authors confirm that they have no competing interests.

**References**

1. Wang FS, Fan JG, Zhang Z, Gao B and Wang HY: The global burden of liver disease: The major impact of China. Hepatology 60: 2099-2108, 2014.
2. Chen Q, Zhan Q, Li Y, Sun S, Zhao L, Zhang H and Zhang G: Schisandra lignan extract protects against carbon tetrachloride-induced liver injury in mice by inhibiting oxidative stress and regulating the nf-kb and Jnk signaling pathways. Evid Based Complement Alternat Med 2017: 5140297, 2017.
3. Shi H, Han W, Ren F, Chen D, Chen Y and Duan Z: Augmenter of liver regeneration protects against carbon tetrachloride-induced liver injury by promoting autophagy in mice. Oncotarget 8: 12637-12648, 2017.
4. Ren F, Zhang L, Zhang X, Shi H, Wen T, Bai L, Zheng S, Chen Y, Chen D, Li L and Duan Z: Inhibition of glycogen synthase kinase 3β promotes autophagy to protect mice from acute liver failure mediated by peroxisome proliferator-activated receptor α. Cell Death Dis 7: e2151, 2016.
5. Schegg B, Hulsmeier AJ, Rutschmann C, Maag C and Hennet T: Core glycosylation of collagen is initiated by two beta(1-O) galactosyltransferases. Mol Cell Biol 29: 943-952, 2009.
6. Webster JA, Yang Z, Kim YH, Loo D, Mosa RM, Li H and Chen C: Collagen beta (1-O) galactosyltransferase 1 (GLT25D1) is required for the secretion of high molecular weight adiponectin and affects lipid accumulation. Biosci Rep 37: pii: BSR20170105, 2017.
7. Baumann S and Hennet T: Collagen accumulation in osteosarcoma cells lacking GLT25D1 collagen galactosyltransferase. J Biol Chem 291: 18514-18524, 2016.
8. Ku NO, Strnad P, Zhong BH, Tao GZ and Omary MB: Keratins let liver live: Mutations predispose to liver disease and crosslinking generates Mallory-Denk bodies. Hepatology 46: 1639-1649, 2007.
9. Ku NO, Toivola DM, Strnad P and Omary MB: Cytoskeletal keratin glycosylation protects epithelial tissue from injury. Nat Cell Biol 12: 876-885, 2010.
10. Wang C, Kovanen V, Raudasoja P, Eskelinen S, Pospiech H and Myllyla R: The glycosyltransferase activities of lysyl hydroxylase 3 (LH3) in the extracellular space are important for cell growth and viability. J Cell Mol Med 13: 508-521, 2009.
11. Louis H, Van Laethem JL, Wu W, Quertinmont E, Degraef C, Van den Berg K, Demols A, Goldman M, Le Moine O, Geerts A and Devière J: Interleukin-10 controls neutrophilic infiltration, hepatocyte proliferation, and liver fibrosis induced by carbon tetrachloride in mice. Hepatology 28: 1607-1615, 1998.
12. Li R, Wang Y, Zhao E, Wu K, Li W, Shi L, Wang D, Xie G, Yin Y, Deng M, *et al*: Maresin 1, a proresolving lipid mediator, mitigates carbon tetrachloride-induced liver injury in mice. Oxid Med Cell Longev 2016: 9203716, 2016.
13. Livak KJ and Schmittgen TD: Analysis of relative gene expression data using real-time quantitative PCR and the 2(-Delta Delta C(T)) method. Methods 25: 402-408, 2001.
14. Nitta T, Kim JS, Mohuczy D and Behrns KE: Murine cirrhosis induces hepatocyte epithelial mesenchymal transition and alterations in survival signaling pathways. Hepatology 48: 909-919, 2008.
15. Li P, Liu S, Lu M, Bandyopadhyay G, Oh D, Imamura T, Johnson AM, Sears D, Shen Z, Cui B, *et al*: Hematopoietic-derived galectin-3 causes cellular and systemic insulin resistance. Cell 167: 973-984 e912, 2016.
16. Goncalves LA, Vigario AM and Penha-Goncalves C: Improved isolation of murine hepatocytes for in vitro malaria liver stage studies. Malar J 6: 169, 2007.
17. Tong J, Yao X, Zeng H, Zhou G, Chen Y, Ma B and Wang Y: Hepatoprotective activity of flavonoids from Cichorium glandulosum seeds in vitro and in vivo carbon tetrachloride-induced hepatotoxicity. J Ethnopharmacol 174: 355-363, 2015.
18. Lucendo-Villarin B, Khan F, Pernagallo S, Bradley M, Iredale JP and Hay DC: Maintaining hepatic stem cell gene expression on biological and synthetic substrata. BioRes Open Access 1: 50-53, 2012.
19. Arriazu E, Ruiz de Galarreta M, Cubero FJ, Varela-Rey M, Perez de Obanos MP, Leung TM, Lopategi A, Benedicto A, Abraham-Enachescu I and Nieto N: Extracellular matrix and liver disease. Antioxid Redox Signal 21: 1078-1097, 2014.

20. Duarte S, Baber J, Fujii T and Coito AJ: Matrix metalloproteinases in liver injury, repair and fibrosis. Matrix Biol 44-46: 147-156, 2015.
21. Fausto N, Campbell JS and Riehle KJ: Liver regeneration. J Hepatol 57: 692-694, 2012.
22. Mizuoka H, Shikata N, Yang J, Takasu M, Inoue K and Tsubura A: Biphasic effect of colchicine on acute liver injury induced by carbon tetrachloride or by dimethylnitrosamine in mice. J Hepatol 31: 825-833, 1999.
23. Pritchard DJ, Wright MG, Sulsh S and Butler WH: The assessment of chemically induced liver injury in rats. J Appl Toxicol 7: 229-236, 1987.
24. Guicciardi ME and Gores GJ: Apoptosis: A mechanism of acute and chronic liver injury. Gut 54: 1024-1033, 2005.
25. Yang BY, Zhang XY, Guan SW and Hua ZC: Protective effect of procyanidin B2 against CCl4-induced acute liver injury in mice. Molecules 20: 12250-12265, 2015.
26. Karakus E, Karadeniz A, Simsek N, Can I, Kara A, Yildirim S, Kalkan Y and Kisa F: Protective effect of Panax ginseng against serum biochemical changes and apoptosis in liver of rats treated with carbon tetrachloride (CCl4). J Hazard Mater 195: 208-213, 2011.
27. Zhang F, Wang X, Qiu X, Wang J, Fang H, Wang Z, Sun Y and Xia Z: The protective effect of Esculentoside A on experimental acute liver injury in mice. PLoS One 9: e113107, 2014.
28. Zeng B, Su M, Chen Q, Chang Q, Wang W and Li H: Protective effect of a polysaccharide from anoectochilus roxburghii against carbon tetrachloride-induced acute liver injury in mice. J Ethnopharmacol 200: 124-135, 2017.
29. Guo J and Friedman SL: Hepatic fibrogenesis. Semin Liver Dis 27: 413-426, 2007.
30. Chanmee T, Ontong P and Itano N: Hyaluronan: A modulator of the tumor microenvironment. Cancer Lett 375: 20-30, 2016.
31. McCracken JM, Jiang L, Deshpande KT, O'Neil MF and Pritchard MT: Differential effects of hyaluronan synthase 3 deficiency after acute vs chronic liver injury in mice. Fibrogenesis Tissue Repair 9: 4, 2016.
32. Shirasaki T, Honda M, Shimakami T, Murai K, Shiomoto T, Okada H, Takabatake R, Tokumaru A, Sakai Y, Yamashita T, *et al*: Impaired interferon signaling in chronic hepatitis C patients with advanced fibrosis via the transforming growth factor beta signaling pathway. Hepatology 60: 1519-1530, 2014.
33. Dooley S and ten Dijke P: TGF-β in progression of liver disease. Cell Tissue Res 347: 245-256, 2012.
34. Macias-Silva M, Abdollah S, Hoodless PA, Pirone R, Attisano L and Wrana JL: MADR2 is a substrate of the TGFbeta receptor and its phosphorylation is required for nuclear accumulation and signaling. Cell 87: 1215-1224, 1996.
35. Niu L, Cui X, Qi Y, Xie D, Wu Q, Chen X, Ge J and Liu Z: Involvement of TGF-β1/smad3 signaling in carbon tetrachloride-induced acute liver injury in mice. PLoS One 11: e0156090, 2016.